East Tennessee State University

Digital Commons @ East Tennessee State University

12-7-2018

Phosphorothioate-Modified AP613-1 Specifically Targets GPC3 When Used for Hepatocellular Carcinoma Cell Imaging

Lili Dong
Fudan University

Hongxin Zhou
Fudan University

Menglong Zhao
Fudan University

Xinghui Gao
Fudan University

Yang Liu
Fudan University

See next page for additional authors

Follow this and additional works at: https://dc.etsu.edu/etsu-works

Citation Information

Phosphorothioate-Modified AP613-1 Specifically Targets GPC3 When Used for Hepatocellular Carcinoma Cell Imaging

Copyright Statement

Creative Commons License

Creator(s)

Lili Dong, Hongxin Zhou, Menglong Zhao, Xinghui Gao, Yang Liu, Dongli Liu, Wei Guo, Hongwei Hu, Qian Xie, Jia Fan, Jiang Lin, and Weizhong Wu

AMERICAN SOCIETY of
GENE & CELL
THERAPY

Phosphorothioate-Modified AP613-1 Specifically Targets GPC3 when Used for Hepatocellular Carcinoma Cell Imaging

Lili Dong,[1,9] Hongxin Zhou,[1,9] Menglong Zhao,[2,9] Xinghui Gao,[3] Yang Liu,[1] Dongli Liu,[1,4] Wei Guo,[3] Hongwei Hu,[5] Qian Xie,[6] Jia Fan,[1,7] Jiang Lin,[2,8] and Weizhong Wu[1]

[1]Liver Cancer Institute, Zhongshan Hospital, Fudan University, Key Laboratory of Carcinogenesis and Cancer Invasion, Ministry of Education, Shanghai 200032, China; [2]Department of Radiology and Shanghai Institute of Medical Imaging, Zhongshan Hospital, Fudan University, Shanghai 200032, China; [3]Department of Laboratory Medicine, Zhongshan Hospital, Fudan University, Shanghai 200032, China; [4]Department of Radiation Oncology, Shanghai General Hospital, Shanghai Jiaotong University, Shanghai 200080, China; [5]Shanghai Aijin Biochemical Science & Technology Co. Ltd., Shanghai 200336, China; [6]Center of Excellence in Inflammation, Infectious Disease and Immunity, James H. Quillen College of Medicine, East Tennessee State University, Johnson City, TN 37614, USA; [7]Institute of Biomedical Sciences, Fudan University, Shanghai 200032, China; [8]Institute of Functional and Molecular Medical Imaging, Fudan University, Shanghai 200040, China

Glypican-3 (GPC3), the cellular membrane proteoglycan, has been established as a tumor biomarker for early diagnosis of hepatocellular carcinoma (HCC). GPC3 is highly expressed in more than 70% HCC tissues detected by antibody-based histopathological systems. Recently, aptamers, a short single-strand DNA or RNA generated from systematic evolution of ligands by exponential enrichment (SELEX), were reported as potential alternatives in tumor-targeted imaging and diagnosis. In this study, a total of 19 GPC3-bound aptamers were successfully screened by capillary electrophoresis (CE)-SELEX technology. After truncated, AP613-1 was confirmed to specifically target GPC3 with a dissociation constant (K_D) of 59.85 nM. When modified with a phosphorothioate linkage, APS613-1 targeted GPC3 with a K_D of 15.48 nM and could be used as a specific probe in living Huh7 and PLC/PRF/5 imaging, GPC3-positive cell lines, but not in L02 or A549, two GPC3-negative cell lines. More importantly, Alexa Fluor 750-conjugated APS613-1 could be used as a fluorescent probe to subcutaneous HCC imaging in xenograft nude mice. Our results indicated that modified AP613-1, especially APS613-1, was a potential agent in GPC3-positive tumor imaging for HCC early diagnosis.

INTRODUCTION

Hepatocellular carcinoma (HCC) is a common malignant cancer worldwide. Several molecules have been used as tumor biomarkers for HCC diagnosis in clinic. Besides AFP, glypican-3 (GPC3), also called DGSX, GTR2-2, MXR7, OCI-5, SDYS, SGB, or SGBS, is the one that is highly expressed in more than 70% of HCC patients.[1] Although lowly expressed in melanoma, ovarian clear cell carcinoma, yolk sac tumors, neuroblastoma, and hepatoblastoma, it is silenced in breast cancer, mesothelioma, epithelial ovarian cancer, lung adenocarcinoma, cholangiocarcinoma (CCA), and normal liver tissues.[2] Therefore, GPC3 might be an ideal tumor biomarker for *in vivo* HCC diagnosis, especially for HCC-targeted imaging.

The level of GPC3 in serum or tumor tissues is usually detected by antibody-based ELISA and previously by immunohistochemical staining. However, some obvious defects of antibody have limited its wide use *in vivo* due to its high immunogenicity, easy degradation, and high cellular cytotoxicity effect. Therefore, a novel reagent needs to be developed as a surrogate in clinical practice. Aptamer[3,4] is a kind of agent, which can specifically target varieties of polypeptides,[5] proteins,[6] and living cells,[7] with high affinity and selectivity by virtue of its topological secondary or tertiary structure. More importantly, aptamers exhibit numerous advantages, such as easy synthetization and chemical modification, high stability, non-toxicity, and non-immunogenicity.[8–11] Thus, aptamers are expected to have great *in vivo* application in cancer diagnosis.

By far, to our knowledge, several aptamers against HCC cells have been reported, such as AS1411, a specific nucleolin-bound aptamer,[12,13] and a series of 6-nt aptamers, which targeted GPC3 and were isolated by cell-systematic evolution of ligands by exponential enrichment (SELEX) containing four standard nucleobases and two added nucleobases (2-amino-8H-imidazo[1,2-a]triazin-4-one and 6-amino-5-nitropyridin-2-one, trivially Z and P), with dissociation constants (K_D) in the range of 6–500 nM.[14] The former was able to suppress HCC by upregulating Galectin-14, and the latter could distinguish cells that expressed GPC3 protein from those that did

not. Here, we first screened GPC3-bound single-stranded DNA (ssDNA) aptamers based on capillary electrophoresis (CE)-SELEX, then we truncated and modified candidates with locked nucleic acid (LNA) substitution and phosphorothioate linkage, and we evaluated their binding affinities on GPC3-positive and GPC3-negtive cells. AP613-1 was found specifically targeting GPC3-positive cells with a high affinity. After LNA substitution and phosphorothioate linkage, the aptamer, especially APS613-1, showed significantly increased affinity with a K_D of 15.48 nM on GPC3-positive cells. In vivo imaging showed that tumor-specific fluorescent signals were clearly observed at nude mice upon HCC xenograft using Alexa Fluor 750-conjugated APS613-1 at 150 min after tail veil injection. Taken together, these results suggested that APS613-1 could be used as a probe for GPC3-positive HCC imaging in vivo.

RESULTS

Characterization of Aptamer-Binding Motif against GPC3

Based on our established screening method,[15] GPC3-bound aptamers were isolated by 6 rounds of CE-SELEX in this study (Figure S1). Finally, 19 aptamers with different nucleic acid sequences were cloned and sequenced (Table S1).

To evaluate the affinities of the screened aptamers, Huh7, a GPC3-positive cell line (Figure S2), was recruited to analyze its fluorescence intensity after incubation with 1 μM FAM-labeled aptamer candidates, one by one, using flow cytometry. Our results showed that 14 of 19 aptamers, such as AP602, AP603, and AP612, exhibited higher binding abilities than that of the initial Library aptamer, suggesting their superior affinities to GPC3 protein expressed on HCC cells. Meanwhile 5 other aptamers, AP631, AP634, AP652, AP657, and AP691, had weakly increased binding abilities compared to the Library control (Figure 1A). After a negative selection with L02, a GPC3-negative cell line (Figure S2), 12 aptamers except AP618 and AP658 had over twice the fluorescent signals in Huh7 cells than those in L02 cells. Among them, AP613, AP625, AP636, AP643, and AP684 were the top 5 aptamers whose fluorescence intensities in Huh7 cells were significantly higher than others (Figure 1B; p < 0.001), indicating that these 5 aptamers had specific and robust GPC3-binding abilities in living HCC cells.

To identify GPC3-binding motifs, the secondary structures of AP613, AP625, AP636, AP643, and AP684 were predicted by DNAMAN software first (Figure 1C), and 7 truncated aptamers with the same characteristic sequences as full-length ones were synthesized thereafter (Figure S3; Table S2). For example, AP613-1, a truncated form of AP613, included a two-small-arm structure (red), while AP636-1 (red) and AP636-2 (blue), two truncated forms of AP636, both contained a long stem-loop structure (Figure 1C). Then, the affinities of 5 full-length aptamers and 7 corresponding truncated ones to GPC3 were analyzed in parallel by flow cytometry in Huh7 and L02 cells. As presented in Figure 1D, the fluorescence intensities of AP613-1 were remarkably enhanced, nearly 2 times those with AP613 in the Huh7 cell line (p < 0.05). The other 6 truncated forms showed no obvious changes in fluorescence intensity when compared with their corresponding full-length aptamers. Thus, AP613-1 was a unique candidate with increased GPC3-binding affinity for this study.

Increased Affinity and Specificity of Modified AP613-1

To protect aptamers from nuclease degradation and promote the affinity in the in vivo context, two types of chemical modifications on AP613-1 nucleotides were introduced in the study. APL613-1 was produced when AP613-1 was modified with three LNA substitutions in the "+" position, and APS613-1 was obtained when three phosphorothioate linkages were at both nucleotide ends in the "*" position (Figure 2A). Then the binding abilities of FAM-labeled AP613, AP613-1, APL613-1, and APS613-1 to Huh7 cells were evaluated once more by flow cytometry. As presented in Figure 2B, the fluorescent signals of APS613-1 and APL613-1 were much stronger than those of AP613, AP613-1, as well as the Library control, indicating that chemically modified AP613-1 exhibited an ascending affinity on GPC3-positive cells, especially of phosphorothioate linkage.

To quantitatively determine the affinities of AP613 and its derivatives, Huh7 cells were incubated with 0, 5, 25, 100, and 500 nM FAM-labeled AP613 and its derivatives, respectively. Then the dissociation constant K_D was calculated by nonlinear regression analysis. As shown in Figures 2C and 2D, the K_D of APS613-1, APL613-1, AP613-1, AP613, and the Library control were 15.48 ± 2.96 nM, 34.90 ± 9.59 nM, 59.85 ± 15.39 nM, 89.30 ± 19.08 nM, and 192.5 ± 70.6 nM, respectively. APS613-1, but not APL613-1, had a significantly lower K_D than those of the other three groups (p < 0.05). That is to say, APS613-1 had the highest affinity to GPC3-expressed cells.

To identify GPC3-binding specificity of APS613-1, GPC3-positive Huh7 and PLC/PRF/5 cell lines,[2] as well as GPC3-negative L02 and A549 cells (Figure S2), were incubated with FAM-labeled APS613-1. Our results showed that APS613-1 had similar K_D on L02 (134.8 ± 49.7 nM) and A549 cells (128.1 ± 41.3 nM), which were almost 8- and 4-fold higher than those of Huh7 (15.48 ± 2.96 nM) and PLC/PRF/5 cells (33.15 ± 6.52 nM), respectively (Figures 2E and S4), manifesting that APS613-1 could recognize GPC3-expressed cells distinctively.

HCC Cell Imaging with APS613-1

To explore the potential usage of APS613-1 in HCC imaging, direct fluorescent stainings on Huh7, PLC/PRF/5, L02, and A549 cells, as well as HCC and adjacent noncancerous tissues, were done using FAM-labeled APS613-1. As expected, intensive fluorescent signals were observed on the cytomembrane of Huh7 and PLC/PRF/5 cells, yet scarcely on those of L02 and A549 cells (Figures 3A and S5). Similar results were achieved when the cells were stained by anti-GPC3 antibody (Figures 3B and S5). In addition, we performed a transient transfection with pcDNA3.1-GPC3[WT] plasmid in L02 cells. Bright green fluorescent signals were also observed using anti-GPC3 antibody and FAM-labeled APS613-1 around nuclei of L02-GPC3-O cells (Figure 3C). Meanwhile, APS613-1 and anti-GPC3 antibody exhibited similar positive staining in the membrane and cytoplasm in
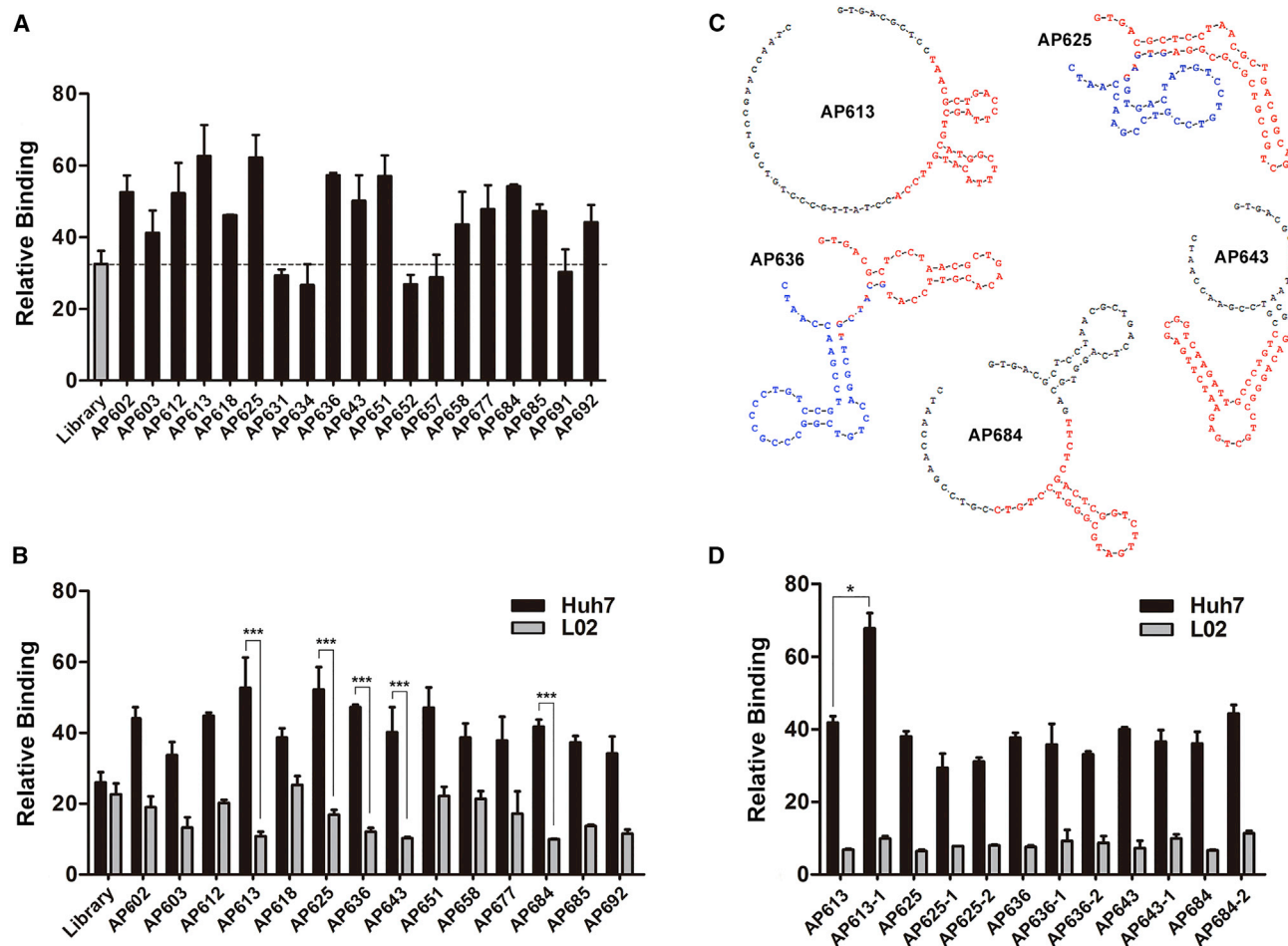
Figure 1. The Affinity and Specificity of Aptamer Candidates

(A) The binding abilities of 19 screened aptamers against GPC3-positive Huh7 cells. 14 aptamers, such as AP602, AP603, AP612, etc., had superior affinities against Huh7 cells than that of the initial Library aptamer. (B) The binding specificities of 14 high-affinity aptamers against Huh7 and GPC3-negative L02 cells. AP613, AP625, AP636, AP643, and AP684 generated over twice stronger fluorescent signals in Huh7 cells than those in L02 cells, and their binding abilities reached significant difference (p < 0.001) between Huh7 and L02 cells. (C) The second structures of the top 5 aptamers with the highest GPC3-binding affinities predicted by DNAMAN. The probable binding motifs with characteristic sequences are highlighted in red or blue. (D) The differential affinities between 5 full-length aptamers and 7 corresponding truncated ones. AP613-1 generated a significant affinity with a nearly 2 times increase to Huh7 cells than that of AP613 (p < 0.05). However, similar binding affinities were found between AP613-1 and AP613 to L02 cells. Data were mean ± SEM and representative of three independent experiments.

human HCC tissues and adjacent noncancerous tissues (Figure 4). However, it should be mentioned that positive nuclear staining appeared in the APS613-1, but not in the anti-GPC3 antibody staining (Figure 4). One probable reason was that APS613-1 aptamer might exhibit more nucleus permeability than that of antibody, resulting in a brighter green staining.

To confirm the specific binding potential of APS613-1 on GPC3, Huh7, PLC/PRF/5, L02-GPC3-O, L02, and A549 cells were first probed with 0.5 μM FAM-labeled APS613-1, and then they were fixed and re-probed with 5 μg/mL antibody against human GPC3. As shown in Figure 5A, most green fluorescent signals were observed on the cytomembrane, and red fluorescent signals were almost observed in the cytoplasm in Huh7, PLC/PRF/5, and L02-GPC3-O cells. Next, when these cells were pre-probed with anti-GPC3 antibody and then fixed and re-probed with FAM-labeled APS613-1, red signals were observed on the cytomembrane and green signals were in the cytoplasm in GPC3-positive cell lines (Figure 5B). Finally, when Huh7, PLC/PRF/5, and L02-GPC3-O cells were fixed with 4% paraformaldehyde and then co-incubated with FAM-labeled APS613-1 and anti-GPC3 antibody, some orange fluorescent signals were observed (Figure 5C), indicating the co-localization of both probes on GPC3 molecules. Therefore, our results revealed that APS613-1 indeed bound GPC3 specifically.

High Stability and Tissue Imaging of APS613-1

To investigate the stability of aptamers, APS613-1 and the Library control were first incubated with human serum, and then they were
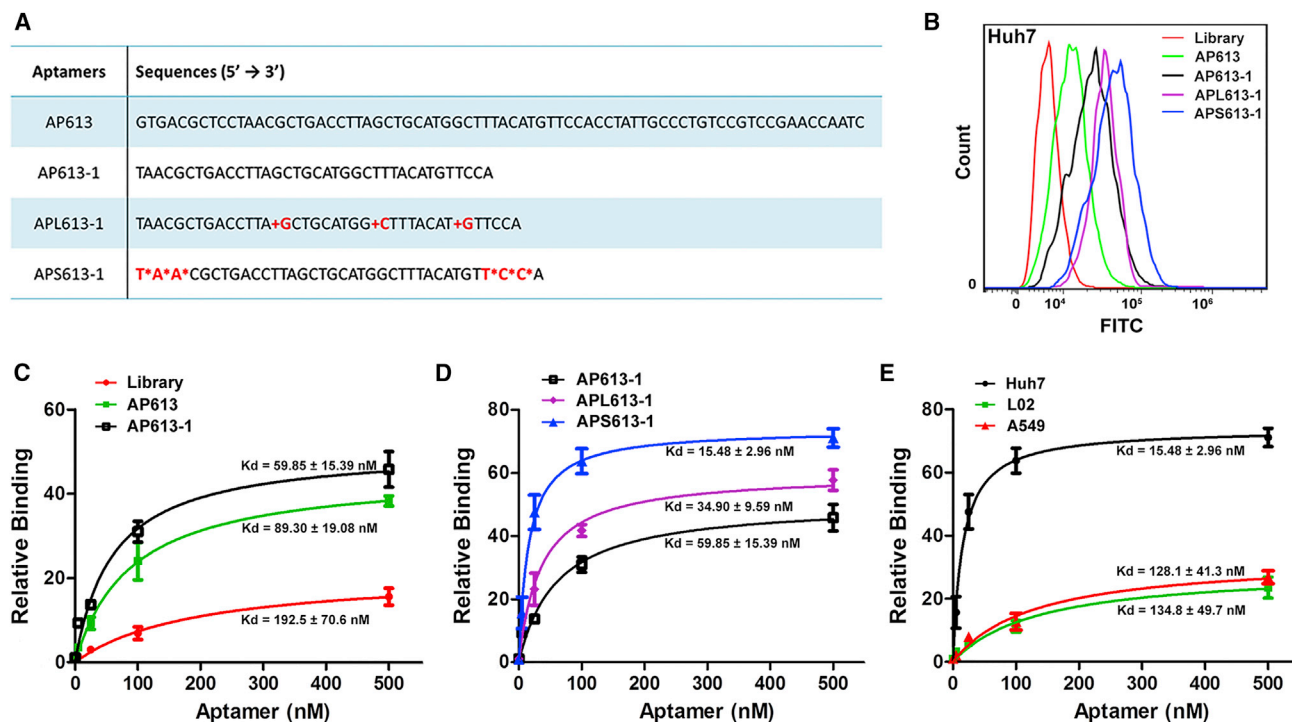
Figure 2. The Affinity and Specificity of Modified AP613-1

(A) Nucleotide sequences and chemical modification. AP613-1 was a truncated form of AP613. APL613-1 had LNA substitution in the "+" positions and APS613-1 was modified with phosphorothioate linkage in the "*" positions. (B) Flow cytometric profiles of AP613, AP613-1, APL613-1, and APS613 as well as the initial Library aptamer binding with Huh7 cells. APS613-1 had the highest fluorescent signals as the peak shifted remarkably from the left to the rightmost. (C and D) The binding curves and dissociation constants (Kds) of APS613-1, APL613-1 AP613-1 (D), AP613, and the Library (D) control were 15.48 ± 2.96 nM, 34.90 ± 9.59 nM, 59.85 ± 15.39 nM, 89.30 ± 19.08 nM, and 192.5 ± 70.6 nM, respectively. APS613-1 had the lowest Kd in all five groups ($p < 0.05$), revealing the highest affinity to GPC3. (E) The Kds of APS613-1 on L02 and A549 cells were 134.8 ± 49.7 nM and 128.1 ± 41.3 nM, respectively, and almost 8-fold higher than that on Huh7 cells (15.48 ± 2.96 nM), manifesting its targeted binding against GPC3. Data were mean $\pm$ SEM and representative of three independent experiments.

analyzed by their degradation rate at 0, 0.5, 1, 2, and 4 hr, respectively. Both APS613-1 and the Library control showed nearly identical bands to initial ones after 4 hr of incubation (Figure 6A). Similar results were also observed in AP613, AP613-1, and APL613-1 after exposure to human serum for 0, 0.5, 1, 2, and 4 hr (Figure S6). These data demonstrated that AP613 and its derivatives were highly resistant to nuclease degradation *in vitro* within 4 hr and probably appropriate to be used in *in vivo* applications.

To evaluate *in vivo* imaging of aptamers in the HCC xenograft model, Alexa Fluor 750-conjugated APS613-1 and the Library control were injected via tail veins of nude mice. Tumor fluorescent images were serially acquired at 0, 5, 30, 60, 90, 120, and 150 min after aptamer injection in unilateral Huh7 xenograft models (Figures 6B and 6C). Both APS613-1 and the Library control were distributed rapidly throughout the body within 5 min (Figure 6C), and the initial fluorescence intensities ($\times 10^8$) of APS613-1 and the Library control at xenograft regions were 8.41 ± 0.74 and 8.77 ± 1.14, respectively (Figure 6D). However, 150 min after injection, the signals ($\times 10^8$) of APS613-1 at xenograft were 2.46 ± 0.26, much

brighter than those of the Library control (0.93 ± 0.31) and background (Figure 6D). The results were also confirmed in sacrificed xenograft tumors and vital organs at 90 min after injection (Figures 6E, S7, and S8). Significantly stronger signals of APS613-1 in tumor than those of the Library control were confirmed, while other vital organs showed no obvious changes. In bilateral xenograft models, tumor fluorescent images were acquired at 0 and 90 min after aptamer injection (Figures 6F–6H). Obviously, the fluorescence intensity ($\times 10^7$) of the Huh7 tumor (Figure 6G, right red circle) was 12.73 ± 1.34, significantly stronger than that of A549 (3.83 ± 0.68; Figure 6G, right green circle) at 90 min after injection with Alexa Fluor 750-conjugated APS613-1. However, when injected with the Library control, the fluorescent signals ($\times 10^7$) of Huh7 and A549 xenografts were 4.75 ± 2.03 and 5.06 ± 0.98, respectively, showing no obvious changes (Figure 6G, left circles). Similar results were confirmed in dissected Huh7 and A549 tumors at 90 min after aptamer injection (Figure 6I).

Taken together, APS613-1 indeed specifically recognized GPC3-positive HCC cells in our *in vivo* and *ex vivo* experiments, and it had the potential to be used in HCC-targeted imaging in the clinic.
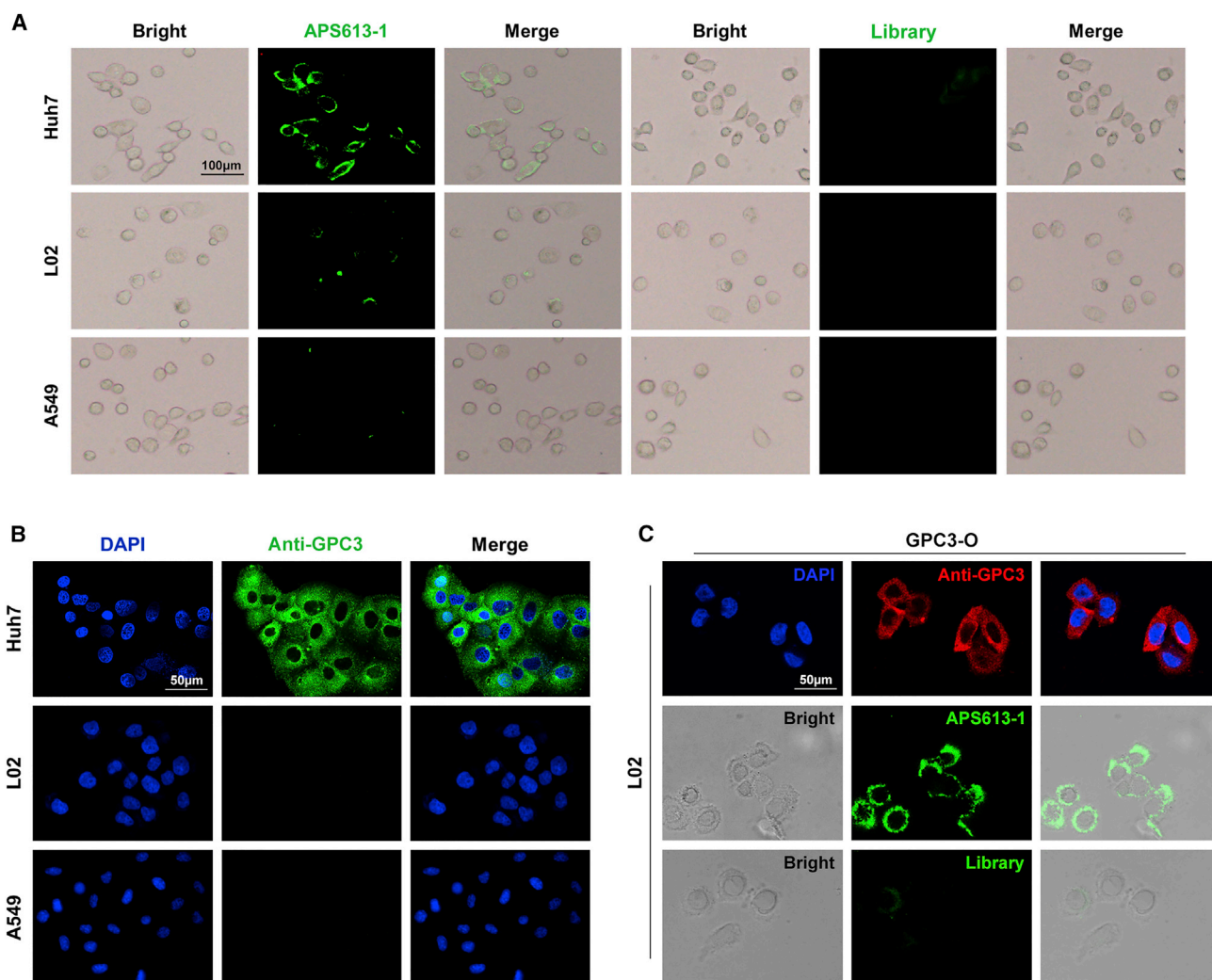
Figure 3. Cell Imaging with APS613-1

(A and B) Fluorescence imaging of Huh7, L02, and A549 cells stained by FAM-labeled APS613-1, FAM-labeled Library control, and anti-GPC3 antibody. (A) Intensive fluorescent signals were observed on the cytomembrane of Huh7 cells, yet scarcely on those of L02 and A549 cells. (B) Similar results were achieved when the cells were stained by anti-GPC3 antibody. (C) Fluorescence imaging of L02-GPC3-O cells stained by anti-GPC3 antibody, FAM-labeled APS613-1, and Library control. Bright green fluorescence was also observed around the nuclei of transfected cells (second row). DAPI was used for contrast staining (blue).

DISCUSSION

HCC is the fourth most common neoplasm worldwide with increasing incidence over the last several decades, and it has the third cancer-related mortality of all human cancers, indicating the poor prognosis of this disease.[16] Due to the asymptomatic nature of HCC in the early stage, patients are often diagnosed in the advanced stages and have considerably lower 5-year survivals than those in the early stage.[2] Surgical resection is one of the few therapeutic options, but only 10%–20% of primary HCCs are resectable at the time of diagnosis. Therefore, it is badly needed to develop a novel and sensitive method for HCC *in vivo* early diagnosis, recurrence monitoring, and prognosis evaluation.

GPC3, a member of the heparan-sulfate proteoglycan (HSPG) family, is highly expressed on cytomembrane through a glycosyl phosphatidylinositol (GPI) anchor in HCC, but not in normal liver tissues.[17] It has been discovered as a sensitively serologic and pathological biomarker for early HCC diagnosis in recent years.[18] Biologically functional studies revealed that GPC3 can stimulate HCC cell growth, migration, and adhesion by upregulating the Wnt-signaling pathway in an autocrine/paracrine manner.[1,19–23] Therefore, GPC3 is also a promising target for *in vivo* HCC imaging and cancer therapy.

At present, the levels of GPC3 in serum and tumor tissues are usually detected by antibody diagnostic systems. Although antibodies are sensitive and specific enough for *in vitro* diagnosis, they are hardly
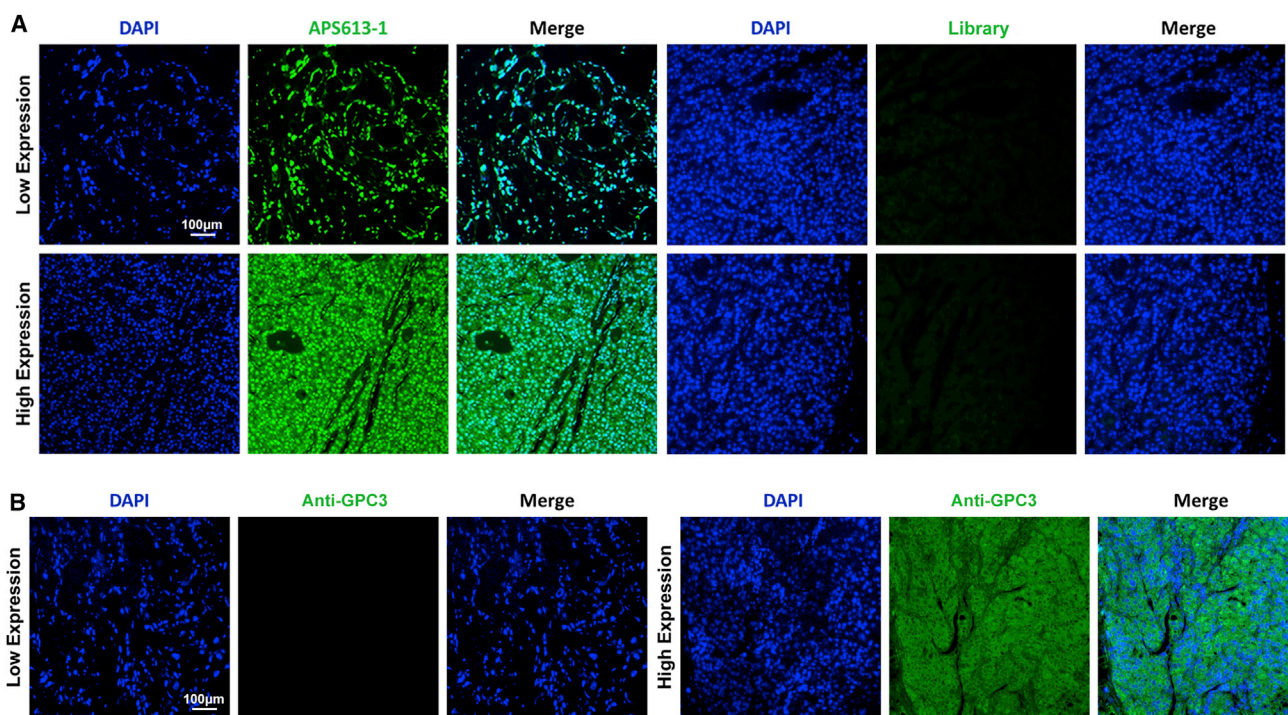
Figure 4. Tissue Imaging with APS613-1

Fluorescence imaging of human hepatocellular carcinomas and adjacent noncancerous tissues stained by FAM-labeled APS613-1 (A), FAM-labeled Library (A), and anti-GPC3 antibody (B). APS613-1 and anti-GPC3 antibody exhibited similar positive staining in the membrane and cytoplasm in human HCC tissues and adjacent noncancerous tissues. DAPI was used for contrast staining (blue).

used *in vivo* due to their high immunogenicity, poor permeability, and instability in the body. By virtue of the secondary or tertiary structures, nucleotide-based aptamers can target a given tumor biomarker with high specificity and affinity like an antibody. More importantly, aptamers have great promise for repeated use in *in vivo* tumor monitoring and imaging by their targeted binding potentials without any obvious antigenicity.

It has been reported that CE-SELEX was an efficient, high-resolving, and time-saving strategy in aptamer screening.[24,25] Indeed, after a four-round selection, we successfully obtained aptamers specifically targeting GPC3 protein. However, GPC3-bound aptamers were dramatically enriched, and their nucleotide sequences were largely homologized after another two-round screening. Some aptamers had even a single base disparity in their nucleotide sequences, for example, AP602 and A603. Therefore, purified PCR products after a six-round CE-SELEX selection were used as the end products for DNA sequencing.

To identify aptamer candidates fitting for HCC *in vivo* imaging, all 19 screened aptamers were first evaluated for their affinities and specificities *in vitro* using several cell lines. By comparing the differences of affinity from a given aptamer between GPC3-positive and GPC3-negative cells, AP613, AP625, AP636, AP643, and AP684 were finally picked out with enormously high affinities to GPC3-postive HCC cells.

Like antibody, not every nucleotide in one aptamer is required for its binding motif composition.[26–28] Some may be necessary for the secondary structure formation or maintenance. To identify the minimal binding motif, an aptamer would be truncated to abbreviate all unnecessary nucleotide sequences without compromising its binding specificity and affinity. Some strategies, such as partial hydrolysis and footprinting[29–31] used for the protein-binding motif analysis, were not apt to nucleotide-binding motif analysis in aptamers. With the development of bioinformatics, the secondary structure, as well as the binding motif of aptamers, could be easily predicted.[26,27,32,33] In theory, any truncated aptamer, with a binding motif in the same secondary structure as the full-length ones, would be the same or similar in its binding specificity but vary in its affinity. Therefore, the motifs of the top 5 GPC3-bound aptamers were predicted, truncated, and then re-evaluated in the study. Our preliminary results showed that predicted motifs based on the secondary structure were often empirical and sometimes unreliable. More parameters, such as charges or advanced structures of aptamers, should be considered during motif analysis.

To prevent rapid nuclease degradation and promote affinity *in vivo*, aptamers are usually subjected to modification. After being substituted or encapsulated with different chemical groups, the advanced structures and their *in vivo* stabilities of aptamers are significantly optimized. LNAs are similar to traditional bases, but they have
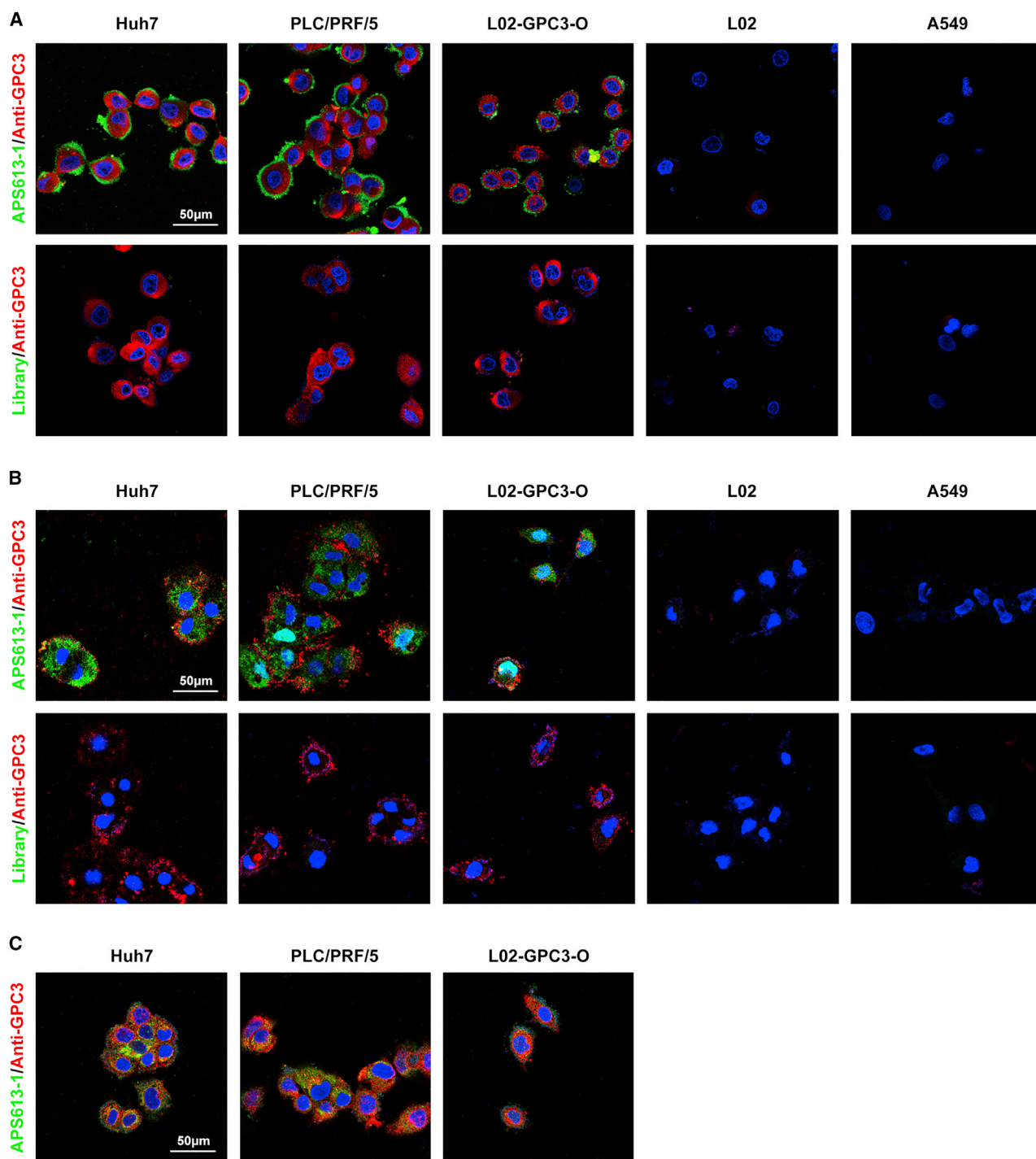
Figure 5. Colocalization Analysis of APS613-1 to GPC3 with Anti-GPC3 Antibody

(A) Fluorescence imaging of Huh7, PLC/PRF/5, L02-GPC3-O, L02, and A549 cells stained by FAM-labeled APS613-1 first, and then fixed and re-stained by anti-GPC3 antibody. Most green fluorescent signals were observed on the cytomembrane and red fluorescent signals were almost observed in the cytoplasm in Huh7, PLC/PRF/5, and L02-GPC3-O cells. (B) Fluorescence imaging of Huh7, PLC/PRF/5, L02-GPC3-O, L02, and A549 cells stained by anti-GPC3 antibody first, and then fixed and re-stained by FAM-labeled APS613-1. Red signals were observed on the cytomembrane, and green signals in the cytoplasm in GPC3-positive cell lines. (C) Fluorescence imaging of Huh7, PLC/PRF/5, and L02-GPC3-O cells co-incubated with FAM-labeled APS613-1 and anti-GPC3 antibody after being fixed with 4% paraformaldehyde. Some orange fluorescent signals were observed.
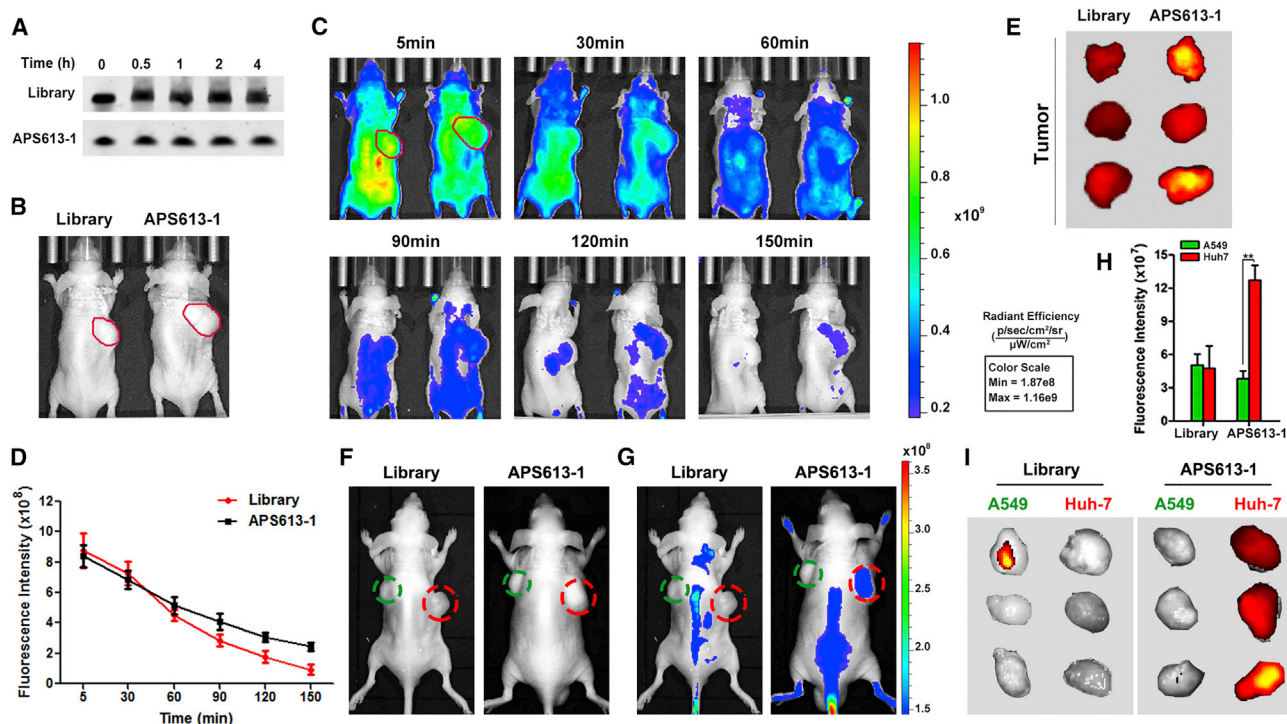
Figure 6. Nuclease Stability and *In Vivo* Imaging with APS613-1 in Nude Mice

(A) Nuclease stability of the Library and APS613-1 with human serum at 0, 0.5, 1, 2, and 4 hr. They both showed nearly identical bands to initial ones after 4 hr of incubation. (B) Imaging of dorsal side of live mice before injection. Unilateral Huh7 tumor site is circled in red. (C) *In vivo* fluorescent images of Huh7 tumors in live mice after injection with Alexa Fluor 750-conjugated Library and APS613-1 at 5, 30, 60, 90, 120, and 150 min, respectively. Both APS613-1 and the Library control were distributed rapidly throughout the mice within 5 min, including tumor sites. At 150 min after injection, the fluorescent signals of APS613-1 at tumor sites became brighter than those of nontarget tissues. Meanwhile, almost no signals were observed in the Library control. (D) Fluorescence intensities of ROIs after injection with Alexa Fluor 750-conjugated Library and APS613-1 at 5, 30, 60, 90, 120, and 150 min, respectively. At 5 min, the fluorescence intensities ($\times 10^8$) of tumor regions of the Library control and APS613-1 were 8.77 ± 1.14 and 8.41 ± 0.74, respectively. At 150 min after injection, the fluorescence intensities ($\times 10^8$) were reduced to 0.93 ± 0.31 and 2.46 ± 0.26, respectively (n = 3). The Library control declined even faster than APS613-1. (E) Fluorescence imaging of Huh7 tumor tissues after mouse dissection. Much brighter signals of APS613-1 were confirmed than those of the Library control at 90 min after injection. (F) Imaging of the dorsal side of live mice before injection in bilateral xenograft models. The Huh7 tumor site is circled in red and the A549 tumor site is circled in green. (G) *In vivo* fluorescent images of bilateral tumors in live mice after injection with Alexa Fluor 750-conjugated Library and APS613-1 at 90 min. The fluorescence intensity of the Huh7 tumor (right red circle) was stronger than that of the A549 (right green circle) after injection with APS613-1, while the models injected with the Library control showed no obvious changes (left circles). (H) Fluorescence intensities of ROIs at 90 min after injection with Alexa Fluor 750-conjugated Library and APS613-1 in bilateral xenograft models. In the APS613-1 group, the fluorescence intensity ($\times 10^7$) of the Huh7 tumor was 12.73 ± 1.34, significantly higher than that of the A549 (3.83 ± 0.68, n = 3). The signals ($\times 10^7$) of the Huh7 and A549 xenografts injected with the Library control were 4.75 ± 2.03 and 5.06 ± 0.98, respectively (n = 3). (I) Fluorescence imaging of Huh7 and A549 tumor tissues after mouse dissection. Much brighter signals of the Huh7 tumors were confirmed than those of the A549 at 90 min after injection with APS613-1, but there was no intensity difference in the Library group between Huh7 and A549 tumors.

a methylene bridge connecting 2′-oxygen of the ribose with 4′-carbon. When incorporating LNA into molecular beacons, the group possesses a 25-fold enhancement in fluorescence signaling.[34] Kubota et al.[35] reported that both the numbers and positions of LNA substitution in the oligonucleotides were the most important factors on DNA stability and affinity. The more LNA substitutes in the central position there were, the higher the binding efficiency of the nucleotide sequence was. In antisense hybridization, oligonucleotides were often modified with phosphorothioate to protect nucleic acid degradation from nuclease. By modifying three to five bases with phosphorothioate at the 5′ and 3′ termini, the oligonucleotides would resist enzymatic degradation dramatically and then significantly increase their stabilities and affinities. So, in this study, three bases in the central po-

sitions of AP613-1 were replaced by LNAs, or three bases at both 5′ and 3′ termini were replaced by phosphorothioates. After chemical modifications, indeed, both APL613-1 and APS613-1, especially the latter, exhibited higher binding abilities to GPC3-positive cells compared to unmodified aptamers.

Next, APS613-1 was tested for its potential application in HCC imaging. As expected, APS613-1 exhibited similar positive staining profiles of HCC cells and tissues like anti-GPC3 antibody. However, some brighter green signals appeared in the nucleus of HCC tissues when probed by APS613-1. To answer the puzzles, Huh7, L02, and A549 cells, after being fixed by 4% paraformaldehyde, were stained with FAM-labeled APS613-1 in parallel. Again, brighter green fluorescent

signals were observed in all nuclei of the 3 cell lines, as well as in the membrane and cytoplasm of Huh7, but not in L02 and A549, cells (Figure S9). A strong positive nuclear staining also was observed in paraformaldehyde-fixed Huh7 cells with AP613-1, not AP613 (Figure S10). All these results indicated that nuclear staining of aptamers might be nonspecific and independent of GPC3 levels, cell types, and chemically modified patterns but probably dependent on membrane penetrability increased by paraformaldehyde fixation and molecular weights of the probes. That is to say, the truncated form of the aptamer, APS613-1, was probably more fitting for living HCC imaging.

Considering the superior properties of aptamers in targeted imaging *in vivo*, Alexa Fluor 750-conjugated APS613-1 was explored for *in vivo* HCC imaging in nude mice. Subcutaneous Huh7 xenografts were indeed specifically imaged at 150 min after APS613-1 injection, suggesting the aptamer could be a novel agent for GPC3-positive HCC imaging. However, orthotopic Huh7 xenografts in nude mouse were difficult to detect because of the poor penetration of fluorescent signals in deep tissues. Therefore, APS613-1 conjugated with other agents, such as magnetic nanoparticles (e.g., Fe_3O_4) or ^{18}F, would be more pragmatic in the clinical setting when used for *in vivo* HCC imaging on an MRI or positron emission tomography/computed tomography (PET-CT) system, with much higher sensitivity and resolution than these with fluorescent imaging.[36–38]

In conclusion, phosphorothioate-modified AP613-1 was a novel specific probe against GPC3, and it is probably a promising agent for *in vivo* GPC3-positive HCC imaging in the future.

MATERIALS AND METHODS

Aptamers and Primers
The initial ssDNA Library, PCR primers, and FAM-conjugated aptamer candidates were chemically synthesized by Sangon Biotech, Shanghai, China. Alexa Fluor 750-conjugated aptamers were synthesized by Thermo Fisher Scientific, Shanghai, China. LNA- and phosphorothioate-modified aptamers were synthesized by Genscript Biotech, Nanjing, China.

The ssDNA Library contained a 35-nt random sequence in the central region, flanked by the 20-nt constant region at the 5′- and 3′ ends, respectively (5′-GTGACGCTCCTAACGCTGAC-N35-CCTGTCCGTCCGAACCAA TC-3′). The primers for the amplification of double-stranded DNA were 5′-GTGACGCTCCTAACGCT GAC-3′ (forward primer, P1) and 5′-GATTGGTTCGGACGGA CAGG-3′ (reverse primer, P2). The biotinylated reverse primer (bio-P2) at the 5′ end was also prepared for the ssDNA sub-Library.

Cell Lines and Cell Culture
Four human cell lines were used in this study: Huh7 and PLC/PRF/5, two liver cancer cell lines with GPC3-positive expression; L02, a normal liver cell line with GPC3-negative expression; and A549, a lung cancer cell line with GPC3-negative expression. All four cell lines were purchased from the Shanghai cell bank of the Chinese Academy of Sciences and cultured in DMEM with high glucose (DMEM-H)

(Gibco Life Technologies, Carlsbad, CA, USA), supplemented with 10% fetal bovine serum (FBS; Gibco).

Vector and Transfection
The pcDNA3.1-GPC3^{WT} plasmid overexpressing GPC3 protein was a gift from Professor Z.J. Chen (Shanghai Institute of Biochemistry and Cell Biology, Shanghai Institute for Biological Science, China). The pcDNA3.1-GPC3^{WT} plasmids were transfected into L02 cells using Lipofectamine 3000 Reagent according to the product manual (Thermo Fisher Scientific, Carlsbad, CA, USA).

CE-SELEX Procedure
GPC3-bound ssDNA candidates were selected as previously described.[15] Simply, purified recombinant human glypican-3 protein (GPC3, R&D Systems, Minneapolis, MN, USA) was mixed with the ssDNA Library (10 μM) at the final concentration of 50 μg/mL and then injected into the capillary. Under the pressure of 0.5 psi and the voltage of −8 kV, GPC3-bound aptamers were separated from unbound ssDNAs, then collected and amplified by routine PCR.

The PCRs were set up in a final volume of 100 μL with 2 μL template described as above, 50 μL 2× Taq PCR MasterMix (Tiangen Biotech, Beijing, China), 0.4 μM P1, and 0.4 μM bio-P2. The reaction was performed at 94°C for 3 min; then 15 cycles of 94°C for 30 s, 58°C for 30 s, and 72°C for 30 s; and, finally, at 72°C for 5 min for extension.

Then the ssDNA sub-Library was separated from the PCR-amplified products using Dynabeads M-280 Streptavidin (Thermo Fisher Scientific).[15] Briefly, about 10 μg PCR products was incubated with 1 mg pre-washed Dynabeads for 20 min. After washing and denaturing, the Dynabead-unbound ssDNAs were precipitated, resuspended, and quantified, which served as the sub-Library ssDNAs for the next round selection.

Cloning and DNA Sequencing
After the sixth round selection, PCR products were purified and cloned using a previously described method.[15] 92 white clones were picked out for nucleic acid sequencing by Sangon. Each was named as AP6XX according to their serial sequencing number.

Secondary Structure Prediction and Modification
The secondary structures of aptamers were predicted by DNAMAN software (version 5.2; Lynnon, Pointe-Claire, QC, Canada). Based on their characteristics of secondary structures, aptamers were truncated only to retain the potential binding motif for the targeted protein. Then, the dominant truncated candidates were further modified with LNA substitution or phosphorothioate linkage.

Flow Cytometry Analysis
The specific affinities of GPC3-bound aptamers were assessed by fluorescence-activated cell sorting (Becton Dickinson, FACScan, Mansfield, MA, USA). Briefly, about 1×10^6 cells were incubated at 37°C for 60 min with various concentrations of 6-carboxy-fluorescein (6-FAM)-labeled aptamer candidates in 200 μL PBS buffer containing

1% BSA. Cells were then washed twice with 0.8 mL PBS buffer to remove unbound ssDNAs and resuspended in 0.5 mL PBS buffer for binding analysis. The fluorescence intensity was analyzed by counting 10,000 events. The initial ssDNA Library was used as a negative aptamer control. L02 and A549 cell lines were used as negative cell controls. Meanwhile, cell staining with 5 μg/mL mouse anti-human GPC3 antibody (Abcam, Cambridge, MA, USA) was performed as a positive GPC3 control. Equilibrium K_D of the aptamer-cell interactions were obtained by fitting the dependence of relative fluorescence intensity of specific binding according to the following equation: $Y = Bmax \times X/(K_D + X)$. Y represented the value of relative binding, Bmax was the maximal value of relative binding, and X was the concentration of the aptamer. All binding assays were repeated three times.

HCC Cell and Tissue Imaging with Aptamers

Cells were seeded into 6-well confocal plates (NEST Biotech, Wuxi, China) at an initial number of 1×10^5 cells/well. After a 24-hr culture, the cells were washed with PBS buffer three times and stained with 0.5 μM FAM-labeled aptamers at 37°C in the dark for 60 min. After thoroughly washing, the cells were imaged by a fluorescence microscope (Olympus, Tokyo, Japan) or laser-scanning confocal microscope (Leica SP8, Leica Microsystems, Richmond Hill, ON, Canada). Meanwhile, immunofluorescence staining using 5 μg/mL rabbit anti-human GPC3 antibody (Abcam) was performed as a positive control. For co-localization analysis, prior to fixation, cells were incubated with labeled aptamers or Anti-GPC3 antibody, and then they were fixed and re-incubated with antibody or aptamers.

Tissue slices with HCC or adjacent noncancerous tissues were preheated at 60°C overnight; deparaffinized in xylene for 10 min twice; and then sequentially immersed in 100%, 95%, 80%, and 75% of ethanol solution at 5-min intervals. After being washed with PBS three times, the slices were treated with 95°C heated buffer (0.01 M citrate buffer [pH 6.0]) for 15 min to retrieve antigen, blocked with PBS buffer containing 5% BSA for 60 min at room temperature, and then incubated with 0.5 μM FAM-labeled aptamers at 37°C for another 60 min. The signals were detected by a fluorescence microscope (Olympus), while the staining of anti-GPC3 antibody (mouse anti-human, 5 μg/mL; Abcam) was performed in parallel as a positive control.

Human Serum Degradation Assay

1 μM candidate aptamer was incubated with human serum (Waryong Biotech, Beijing, China) at 37°C. The reaction was quenched at the indicated time points by adding an equal volume of loading buffer (8 M urea, 20 mM EDTA, 5 mM Tris-HCl [pH 7.5], and 0.25% bromophenol blue). The reaction mixtures were then separated on 10% polyacrylamide/8 M urea gels. The gels were stained with GelRed (Biotium, Hayward, CA, USA) for 30 min before being visualized under a Tanon 3500 Gel Imaging System (Tanon, Shanghai, China).

In Vivo and *Ex Vivo* Tumor Imaging

About 5×10^6 tumor cells were subcutaneously transplanted into the right upper flank (Huh7, n = 6) or bilateral upper flanks (right Huh7, left A549, n = 6) of 4-week-old male BALB/c nude mice. When the xenograft tumor grew to 1–2 cm in diameter, all mice were randomly divided into four groups with three mice per group. About 0.65 nmol Alexa Fluor 750-conjugated experimental or control aptamers in 150 μL PBS buffer were injected into nude mice via a lateral tail vein. Then, at a given time, the fluorescence images of xenograft tumors in the dorsal side of nude mice were taken by the IVIS Lumina XRMS Series III fluorescence imaging system (PerkinElmer, Waltham, MA, USA). The intensities of tumor regions of interest (ROIs) (radiance efficiency, $[p/s/cm^2/sr]/[\mu W/cm^2]$) were generated automatically by Living Image 4.4 software and then analyzed. All animals were kept in a pathogen-free environment and fed ad lib. The procedures for care and use of animals were approved by the Ethics Committee of Zhongshan Hospital of Fudan University (Shanghai, China) and all applicable institutional and governmental regulations concerning the ethical use of animals were followed.

Statistical Analysis

Data were analyzed using GraphPad Prism 5 software. Quantitative variables were expressed as means ± SEM and analyzed by two-way ANOVA and Student's t test. Results were considered statistically significant at $p < 0.05$.

SUPPLEMENTAL INFORMATION

Supplemental Information includes two tables and ten figures and can be found with this article online at https://doi.org/10.1016/j.omtn.2018.09.013.

AUTHOR CONTRIBUTIONS

L.D., H.Z., M.Z., J.L., and W.W. conceived and designed the study. X.G. and W.G. performed CE-related assays. L.D., H.Z., Y.L., and D.L. performed the experiments, including transfection, PCR, cloning, flow cytometry, and immunofluorescence. L.D. performed motifs and structures analysis. H.Z. and M.Z. performed *in vivo* imaging assays. L.D., H.Z., M.Z., J.L., and W.W. analyzed the data and prepared the manuscript. H.H., Q.X., and J.F. participated in study design. All authors read and approved the final manuscript.

CONFLICTS OF INTEREST

The authors have no conflicts of interest.

ACKNOWLEDGMENTS

REFERENCES

1. Zhou, F., Shang, W., Yu, X., and Tian, J. (2017). Glypican-3: A promising biomarker for hepatocellular carcinoma diagnosis and treatment. Med. Res. Rev. *38*, 741–767.

2. Ho, M., and Kim, H. (2011). Glypican-3: a new target for cancer immunotherapy. Eur. J. Cancer *47*, 333–338.

3. Ellington, A.D., and Szostak, J.W. (1990). In vitro selection of RNA molecules that bind specific ligands. Nature *346*, 818–822.

4. Tuerk, C., and Gold, L. (1990). Systematic evolution of ligands by exponential enrichment: RNA ligands to bacteriophage T4 DNA polymerase. Science *249*, 505–510.

5. Ni, X., Zhang, Y., Ribas, J., Chowdhury, W.H., Castanares, M., Zhang, Z., Laiho, M., DeWeese, T.L., and Lupold, S.E. (2011). Prostate-targeted radiosensitization via aptamer-shRNA chimeras in human tumor xenografts. J. Clin. Invest. *121*, 2383–2390.

6. Potty, A.S., Kourentzi, K., Fang, H., Jackson, G.W., Zhang, X., Legge, G.B., and Willson, R.C. (2009). Biophysical characterization of DNA aptamer interactions with vascular endothelial growth factor. Biopolymers *91*, 145–156.

7. Xiao, Z., Shangguan, D., Cao, Z., Fang, X., and Tan, W. (2008). Cell-specific internalization study of an aptamer from whole cell selection. Chemistry *14*, 1769–1775.

8. O'Sullivan, C.K. (2002). Aptasensors–the future of biosensing? Anal. Bioanal. Chem. *372*, 44–48.

9. Gold, L., Ayers, D., Bertino, J., Bock, C., Bock, A., Brody, E.N., Carter, J., Dalby, A.B., Eaton, B.E., Fitzwater, T., et al. (2010). Aptamer-based multiplexed proteomic technology for biomarker discovery. PLoS ONE *5*, e15004.

10. Wang, H.Q., Wu, Z., Tang, L.J., Yu, R.Q., and Jiang, J.H. (2011). Fluorescence protection assay: a novel homogeneous assay platform toward development of aptamer sensors for protein detection. Nucleic Acids Res. *39*, e122.

11. Jenison, R.D., Gill, S.C., Pardi, A., and Polisky, B. (1994). High-resolution molecular discrimination by RNA. Science *263*, 1425–1429.

12. Cho, Y., Lee, Y.B., Lee, J.H., Lee, D.H., Cho, E.J., Yu, S.J., Kim, Y.J., Kim, J.I., Im, J.H., Lee, J.H., et al. (2016). Modified AS1411 Aptamer Suppresses Hepatocellular Carcinoma by Up-Regulating Galectin-14. PLoS ONE *11*, e0160822.

13. Rosenberg, J.E., Bambury, R.M., Van Allen, E.M., Drabkin, H.A., Lara, P.N., Jr., Harzstark, A.L., Wagle, N., Figlin, R.A., Smith, G.W., Garraway, L.A., et al. (2014). A phase II trial of AS1411 (a novel nucleolin-targeted DNA aptamer) in metastatic renal cell carcinoma. Invest. New Drugs *32*, 178–187.

14. Zhang, L., Yang, Z., Le Trinh, T., Teng, I.T., Wang, S., Bradley, K.M., Hoshika, S., Wu, Q., Cansiz, S., Rowold, D.J., et al. (2016). Aptamers against Cells Overexpressing Glypican 3 from Expanded Genetic Systems Combined with Cell Engineering and Laboratory Evolution. Angew. Chem. Int. Ed. Engl. *55*, 12372–12375.

15. Dong, L., Tan, Q., Ye, W., Liu, D., Chen, H., Hu, H., Wen, D., Liu, Y., Cao, Y., Kang, J., et al. (2015). Screening and Identifying a Novel ssDNA Aptamer against Alpha-fetoprotein Using CE-SELEX. Sci. Rep. *5*, 15552.

16. Siegel, R.L., Miller, K.D., and Jemal, A. (2017). Cancer Statistics, 2017. CA Cancer J. Clin. *67*, 7–30.

17. Filmus, J., and Selleck, S.B. (2001). Glypicans: proteoglycans with a surprise. J. Clin. Invest. *108*, 497–501.

18. Hippo, Y., Watanabe, K., Watanabe, A., Midorikawa, Y., Yamamoto, S., Ihara, S., Tokita, S., Iwanari, H., Ito, Y., Nakano, K., et al. (2004). Identification of soluble NH2-terminal fragment of glypican-3 as a serological marker for early-stage hepatocellular carcinoma. Cancer Res. *64*, 2418–2423.

19. Nakatsura, T., Yoshitake, Y., Senju, S., Monji, M., Komori, H., Motomura, Y., Hosaka, S., Beppu, T., Ishiko, T., Kamohara, H., et al. (2003). Glypican-3, overexpressed specifically in human hepatocellular carcinoma, is a novel tumor marker. Biochem. Biophys. Res. Commun. *306*, 16–25.

20. Qi, X.H., Wu, D., Cui, H.X., Ma, N., Su, J., Wang, Y.T., and Jiang, Y.H. (2014). Silencing of the glypican-3 gene affects the biological behavior of human hepatocellular carcinoma cells. Mol. Med. Rep. *10*, 3177–3184.

21. Pez, F., Lopez, A., Kim, M., Wands, J.R., Caron de Fromentel, C., and Merle, P. (2013). Wnt signaling and hepatocarcinogenesis: molecular targets for the development of innovative anticancer drugs. J. Hepatol. *59*, 1107–1117.

22. Capurro, M., Martin, T., Shi, W., and Filmus, J. (2014). Glypican-3 binds to Frizzled and plays a direct role in the stimulation of canonical Wnt signaling. J. Cell Sci. *127*, 1565–1575.

23. Kakugawa, S., Langton, P.F., Zebisch, M., Howell, S., Chang, T.H., Liu, Y., Feizi, T., Bineva, G., O'Reilly, N., Snijders, A.P., et al. (2015). Notum deacylates Wnt proteins to suppress signalling activity. Nature *519*, 187–192.

24. Mendonsa, S.D., and Bowser, M.T. (2004). In vitro evolution of functional DNA using capillary electrophoresis. J. Am. Chem. Soc. *126*, 20–21.

25. Mendonsa, S.D., and Bowser, M.T. (2004). In vitro selection of high-affinity DNA ligands for human IgE using capillary electrophoresis. Anal. Chem. *76*, 5387–5392.

26. Bing, T., Yang, X., Mei, H., Cao, Z., and Shangguan, D. (2010). Conservative secondary structure motif of streptavidin-binding aptamers generated by different laboratories. Bioorg. Med. Chem. *18*, 1798–1805.

27. Shangguan, D., Tang, Z., Mallikaratchy, P., Xiao, Z., and Tan, W. (2007). Optimization and modifications of aptamers selected from live cancer cell lines. ChemBioChem *8*, 603–606.

28. Lyu, Y., Chen, G., Shangguan, D., Zhang, L., Wan, S., Wu, Y., Zhang, H., Duan, L., Liu, C., You, M., et al. (2016). Generating Cell Targeting Aptamers for Nanotheranostics Using Cell-SELEX. Theranostics *6*, 1440–1452.

29. Legiewicz, M., and Yarus, M. (2005). A more complex isoleucine aptamer with a cognate triplet. J. Biol. Chem. *280*, 19815–19822.

30. Manimala, J.C., Wiskur, S.L., Ellington, A.D., and Anslyn, E.V. (2004). Tuning the specificity of a synthetic receptor using a selected nucleic acid receptor. J. Am. Chem. Soc. *126*, 16515–16519.

31. Sayer, N.M., Cubin, M., Rhie, A., Bullock, M., Tahiri-Alaoui, A., and James, W. (2004). Structural determinants of conformationally selective, prion-binding aptamers. J. Biol. Chem. *279*, 13102–13109.

32. Zuker, M. (2003). Mfold web server for nucleic acid folding and hybridization prediction. Nucleic Acids Res. *31*, 3406–3415.

33. Mei, H., Bing, T., Yang, X., Qi, C., Chang, T., Liu, X., Cao, Z., and Shangguan, D. (2012). Functional-group specific aptamers indirectly recognizing compounds with alkyl amino group. Anal. Chem. *84*, 7323–7329.

34. Martinez, K., Estevez, M.C., Wu, Y., Phillips, J.A., Medley, C.D., and Tan, W. (2009). Locked nucleic acid based beacons for surface interaction studies and biosensor development. Anal. Chem. *81*, 3448–3454.

35. Kubota, K., Ohashi, A., Imachi, H., and Harada, H. (2006). Improved in situ hybridization efficiency with locked-nucleic-acid-incorporated DNA probes. Appl. Environ. Microbiol. *72*, 5311–5317.

36. Wang, F.B., Rong, Y., Fang, M., Yuan, J.P., Peng, C.W., Liu, S.P., and Li, Y. (2013). Recognition and capture of metastatic hepatocellular carcinoma cells using aptamer-conjugated quantum dots and magnetic particles. Biomaterials *34*, 3816–3827.

37. Roy, K., Kanwar, R.K., and Kanwar, J.R. (2015). LNA aptamer based multi-modal, Fe3O4-saturated lactoferrin (Fe3O4-bLf) nanocarriers for triple positive (EpCAM, CD133, CD44) colon tumor targeting and NIR, MRI and CT imaging. Biomaterials *71*, 84–99.

38. Roy, K., Kanwar, R.K., and Kanwar, J.R. (2017). Corrigendum to "LNA aptamer based multi-modal, Fe$_3$O$_4$-saturated lactoferrin (Fe$_3$O$_4$-bLf) nanocarriers for triple positive (EpCAM, CD133, CD44) colon tumour targeting and NIR, MRI and CT imaging" [Biomaterials 71C (2015) 84-99]. Biomaterials *138*, 118–120.